

Phase Synchronization of Pressure-Flow Fluctuations: A measure of cerebral autoregulation dynamics

Zhi Chen,¹ Kun Hu,¹ H. Eugene Stanley,¹ Vera Novak,^{2,*} and Plamen Ch. Ivanov^{1,*}

¹*Center for Polymer Studies and Department of Physics,
Boston University, Boston, Massachusetts 02215*

²*Division of Gerontology, Harvard Medical School,
Beth Israel Deaconess Medical Center, Boston, MA 02215 USA*

(Dated: December 23, 2018)

We employ a synchronization method to investigate the relationship between the blood flow velocities (BFV) in the middle cerebral arteries (MCA) and beat-to-beat blood pressure (BP) recorded from a finger in healthy and post-stroke subjects during four different physiologic conditions: supine, head-up tilt, hyperventilation and CO₂ rebreathing in upright position. To evaluate whether instantaneous BP changes are synchronized with changes in the BFV, we compare dynamical patterns in the instantaneous phases of these signals, obtained from the Hilbert transform, as a function of time. We find that in post-stroke subjects the instantaneous phase increments of BP and BFV exhibit well pronounced patterns that remain stable in time for all four physiologic conditions, while in healthy subjects these patterns are different, less pronounced and more variable. Further, we show that the instantaneous phase increments of BP and BFV are cross-correlated even within a single heartbeat cycle. The maximum correlation strength is different between conditions and between the groups. For healthy subjects the amplitude of the cross-correlation function is small and attenuates within 3-5 heartbeats. In contrast, for post-stroke subjects, this amplitude is significantly larger and cross-correlations persist up to 20 heartbeats. These findings provide new insight into the mechanism of cerebral vascular control in healthy subjects, suggesting rapid adjustments (within a heartbeat) of the cerebral BFV to changes in peripheral BP.

PACS numbers: 05.40.-a,87.19.Hh,87.10.+e

I. INTRODUCTION

Cerebral autoregulation (CA) is the ability of cerebral blood vessels to maintain steady cerebral perfusion in response to fluctuations of systemic blood pressure (BP), postural changes or metabolic demands. This regulatory mechanism is known to operate over a range of blood pressure values (e.g. 80 - 150 mm Hg) [1] and on time scales above several heartbeats [2]. The longterm CA compensates for chronic BP elevations and metabolic demands [3]. Ischemic stroke is associated with an impairment of autoregulation [4, 5], that may permanently affect cerebrovascular reactivity to chemical and blood pressure stimuli [6, 7]. With impaired CA, the cerebral blood flow follows BP fluctuations posing a risk of insufficient blood supply to the brain during transient drops in peripheral BP. Therefore, evaluating the effectiveness of CA is of great interest, given the clinical implications.

Traditional experimental methods to probe the mechanism of CA require time-consuming invasive procedures [8, 9] and are focused on long term BP and BFV characteristics such as the mean, lacking descriptors of temporal BP-BFV relationship. To address this problem, an alternative "dynamic" approach has been pro-

posed [10] to quantify CA using transcranial Doppler ultrasound during the transient responses in cerebral blood flow velocity to the rapid BP changes, induced experimentally by thigh cuffs inflation, Valsalva maneuver, tilt-up or a change in posture [3, 11]. The indices from this approach may be more sensitive to indicators of hypoperfusion after stroke [12].

The analytic methods valuating the dynamics of cerebral autoregulation are currently based on mathematical modeling and Fourier transform analysis [32]. The Fourier transform based transfer function method has been widely used [2]. This method calculates a relative cross-spectrum between BFV and BP signals in the frequency domain. Dynamic indices of autoregulation, based on Fourier transform methods presume (i) signal stationarity (i.e., the mean and standard deviation of the signal are invariant under a time shift) and (ii) a linear BFV-BP relationship. However, physiologic signals are often nonstationary reflecting transient changes in the physiologic state [13]. The effect of this nonstationarity on the results obtained from the transfer function analysis, has not been carefully assessed in previous studies.

Here we investigate the dynamics of BP-BFV relationship during the quasi-steady state. While studies traditionally have focused on response in BFV to rapid transient changes in BP [3], we hypothesize that spontaneous physiologic fluctuations during a quasi-steady state may also contain important information about the CA mechanism. To test this hypothesis, we have measured BP and BFV signals from healthy and post-stroke subjects

*VN and PChI contributed equally to this work. VN designed the clinical study, provided data and guidance of the physiological aspects. PChI proposed the analysis method, and guided the computational aspects.

during four physiologic conditions: supine and tilt, hyperventilation, CO₂ rebreathing in upright position. We have applied a novel phase synchronization method to quantify the dynamical BP-BFV relationship in these quasi-steady conditions. Interactions between peripheral circulation (beat-to-beat BP) and cerebral vasoregulation (BFV in the middle cerebral artery MCA) can be modeled as dynamic synchronization of two coupled nonlinear systems. We further hypothesize that the CA mechanism may also involve adjustments in the cerebral vascular tone to spontaneous changes in BP that may be present within a single heartbeat even when the system is in the steady state and there are no significant changes in the mean blood pressure.

The synchronization phenomenon was first observed by Huygens for two coupled pendulum clocks [14], and since then it has been found in many physical and biological systems where two or more coupled subsystems interact [15, 16, 17, 18, 19, 20, 21]. Alternatively, the synchronization may also be triggered by the influence of external noisy or regular fields [22, 23]. In recent years, the concept of synchronization has been widely used to study the coupling of oscillating systems, leading to the discovery of phase synchronization in non-identical coupled systems in which the instantaneous phase is synchronized, while their instantaneous amplitude remains uncorrelated [24, 25, 26, 27].

In this study we evaluate the time-domain characteristics of both the amplitudes and the instantaneous phases of the BFV and BP which can be considered as two interacting subsystems within the CA mechanism. To determine the characteristics of the coupling between BP and BFV in healthy subjects and how they change with stroke, we analyze the cross-correlation between the instantaneous phases of these two signals. We find that this cross-correlation is much stronger for stroke subjects, indicating increased synchronization between BP and BFV, which suggests impaired mechanism of the CA. We compare the results of the synchronization analysis with those obtained from the traditional transfer function method.

II. METHODS

Study Groups

Data were obtained at the Autonomic Nervous System Laboratory at the Department of Neurology at The Ohio State University and at the SAFE (Syncope and Falls in the Elderly) Laboratory at the Beth Israel Deaconess Medical Center at Harvard Medical School. All subjects signed informed consent, approved by the Institutional Review Boards. Demographic characteristics are summarized in Table I. Control group: 11 healthy subjects (age 48.2 ± 8.7 years). Stroke group: 13 subjects with a first minor ischemic stroke (> 2 months after acute onset) (age 52.8 ± 7.1 years). Post-stroke subjects had a documented infarct affecting $< 1/3$ of the vascular territory as determined by MRI or CT with a

minor neurological deficit (Modified Rankin Score scale < 3). The side of the lesion was determined by neurological evaluation and confirmed with MRI and CT. The lesion was in the right hemisphere in 5 of the subjects and in the left hemisphere in 8 of the subjects. Normal carotid Doppler ultrasound study was required for participation. Patients with hemorrhagic strokes, clinically important cardiac disease including major arrhythmias, diabetes and any other systemic illness were excluded. All subjects were carefully screened with a medical history, physical and laboratory examination.

Experimental Protocol

All subjects participated in the following experimental protocol:

- Baseline supine normocapnia: subject rests in supine position for 5 minutes on a tilt table;
- Head-up tilt-upright normocapnia: The tilt table is moved upright to an 80° angle. The subject remains in upright position for 5 minutes and is breathing spontaneously;
- Hyperventilation-upright hypocapnia: the subject is asked to breathe rapidly at ≈ 1 Hz frequency for 3 minutes in an upright position. Hyperventilation induces hypocapnia (reduced carbon dioxide), which is associated with cerebral vasoconstriction;
- CO₂-rebreathing-upright hypercapnia: The subject is asked to breath a mixture of air and 5% CO₂ from rebreathing circuit at a comfortable frequency for 3 minutes in an upright position. CO₂-rebreathing increases carbon dioxide above normal levels and induces hypercapnia, which is associated with vasodilatation.

The mechanism of CA is at least partially related to the coupling between the metabolic demands and oxygen supply to the brain [3]. Carbon dioxide (CO₂) is one of the most potent chemical regulators of cerebral vasoreactivity. Head-up tilt provides both pressure and chemical stimulus - BFV and CO₂ decline in upright position, reflecting the change in intracranial pressure and shifting autoregulatory curve towards lower BP values. There is a linear relationship between CO₂ values and cerebral blood flow: hypocapnia (through hyperventilation) causes vasoconstriction thus decrease the support of blood flow in brain, hypercapnia (through CO₂ rebreathing) causes vasodilatation and increase the support of blood flow in brain [3].

Data Acquisition

The experiments were done in the morning or more than 2 hours after the last meal. The electrocardiogram was measured from a modified standard lead II or III using a Spacelab Monitor (SpaceLab Medical Inc., Issaquah, WA). Beat-to-beat BP was recorded from a finger with a Finapres device (Ohmeda Monitoring Systems, Englewood CO), which is based on a photoplethysmographic volume clamp method. During the study protocol, BP was verified by arterial tonometry. With finger

Variable	Demographic characteristics									
	Control					Stroke				
Men/Women	4/7					7/6				
Age(mean±SD)	48.2 ± 8.7					52.8 ± 8.7				
Race W/AA	10/1					12/1				
Stroke side (Right/Left)	-					5/8				
Group (mean±SD)	Supine		Tilt		Hyperventilation		CO ₂ rebreathing		Statistics (P values)	
	Control	Stroke	Control	Stroke	Control	Stroke	Control	Stroke		
BP (mm Hg)	96.4 ± 20.9	101.0 ± 20.6	93.1 ± 20.1	105.9 ± 22.5	94.2 ± 19.7	105.4 ± 22.0	97.6 ± 21.7	108.8 ± 22.7	0.66*	0.0005 ⁺
BFV-MCAR/Normal side(cm/s)	66.0 ± 18.7	55.2 ± 18.0	57.3 ± 18.1	49.7 ± 18.5	40.3 ± 15.7	39.8 ± 14.9	54.7 ± 21.9	56.3 ± 21.5	< 0.0001*	0.77 ⁺
BFV-MCAL/Stroke side(cm/s)	63.5 ± 19.6	51.1 ± 19.0	54.8 ± 17.1	51.5 ± 19.3	40.8 ± 14.9	41.0 ± 17.9	54.6 ± 21.5	57.4 ± 23.3	< 0.0001*	0.008 ⁺
CO ₂ (mm Hg)	33.5 ± 6.0	37.7 ± 4.9	32.0 ± 3.6	32.5 ± 2.5	21.0 ± 4.5	23.5 ± 8.0	34.6 ± 7.2	33.2 ± 6.5	< 0.0001*	0.28 ⁺
CVR**/Normal side	1.54 ± 0.45	1.96 ± 0.54	1.75 ± 0.53	2.28 ± 0.93	2.68 ± 1.10	3.00 ± 1.28	1.97 ± 0.61	2.17 ± 0.83	0.0001*	0.007 ⁺
CVR-MCAL/Stroke side	1.59 ± 0.56	1.97 ± 0.65	1.79 ± 0.61	2.29 ± 0.83	2.57 ± 0.90	3.04 ± 1.60	1.96 ± 0.56	2.19 ± 0.94	0.0001*	0.01 ⁺

* P value between tests comparisons

+ P value between groups comparisons

** CVR (cerebral vascular resistance) is defined as mean BP/BFV

TABLE I: Demographic characteristics.

position at the heart level and temperature kept constant, the Finapres device can reliably track intraarterial BP changes over prolonged periods of time. Respiratory waveforms were measured with a nasal thermistor. CO₂ was measured from a mask using an infrared end tidal volume CO₂ monitor (Datex Ohmeda, Madison WI). The right and left MCAs were insonated from the temporal windows, by placing the 2-MHz probe in the temporal area above the zygomatic arch using a transcranial Doppler ultrasonography system (MultiDop X4, DWL Neuroscan Inc, Sterling, VA). Each probe was positioned to record the maximal BFV and fixed at a desired angle using a three-dimensional positioning system attached to the light-metal probe holder. Special attention was given to stabilize the probes, since their steady position is crucial for reliable, continuous BFV recordings. BFV and all cardiovascular analog signals were continuously acquired on a beat-to-beat basis and stored for off-line post-processing. Data were visually inspected and occasional extrasystoles and outlier data points were removed using linear interpolation. Fourier transform of the Doppler shift (the difference between the frequency of the emitted signal and its echo (frequency of reflected signal) was used to calculate BFV. BFVs in the MCA correlate with invasive measurements of blood flow with xenon clearance, laser Doppler flux and positron emission tomography. Since MCA diameter is relatively constant under physiological conditions, BFV can be used for blood flow estimates.

Statistical analysis

We use analysis of variance (MANOVA) with 2x4 design for two groups (control and stroke) and four tests (supine, tilt, hyperventilation, and CO₂ rebreathing)

with subjects as nested random effects (JMP version 5 Software Analysis Package, SAS Institute, Cary, NC). For each group and test, we have calculated the mean BP, BFV, cerebral vascular resistance (CVR, calculated by mean BP/BFV) from the right and the left MCAs, CO₂ as well as gain, phase and coherence from transfer function analysis, and on the instantaneous phase cross-correlation results obtained from the synchronization analysis. Mean BFV on the stroke side were obtained from the right MCA in five patients and from the left MCA in 8 patients. Mean BFV from the opposite MCA were considered as a normal side. In the group comparison, we have compared the stroke side BFV for the stroke group to the BFV at the left side MCA for the control group, while the normal side BFV for the stroke group has been compared to the BFV at the right side MCA for the control group.

Transfer function analysis

We first normalize the BFV and BP signals to unit standard deviation to obtain the respective signals $V(t)$ and $P(t)$. We then calculate their respective Fourier transforms $V(f)$ and $P(f)$. In the frequency domain, the coherence function $\gamma^2(f)$ is defined as

$$\gamma^2(f) = \frac{|S_{PV}(f)|^2}{S_{PP}(f)S_{VV}(f)}, \quad (1)$$

where $S_{VV}(f) = |V(f)|^2$, $S_{PP}(f) = |P(f)|^2$ and $S_{PV}(f) = P^*(f)V(f)$ are the power spectrum of $V(t)$, $P(t)$ and the cross-spectrum of $V(t)$ and $P(t)$, respectively. The value of the coherence function $\gamma^2(f)$ varies between 0 and 1. The transfer function $H(f)$ is defined

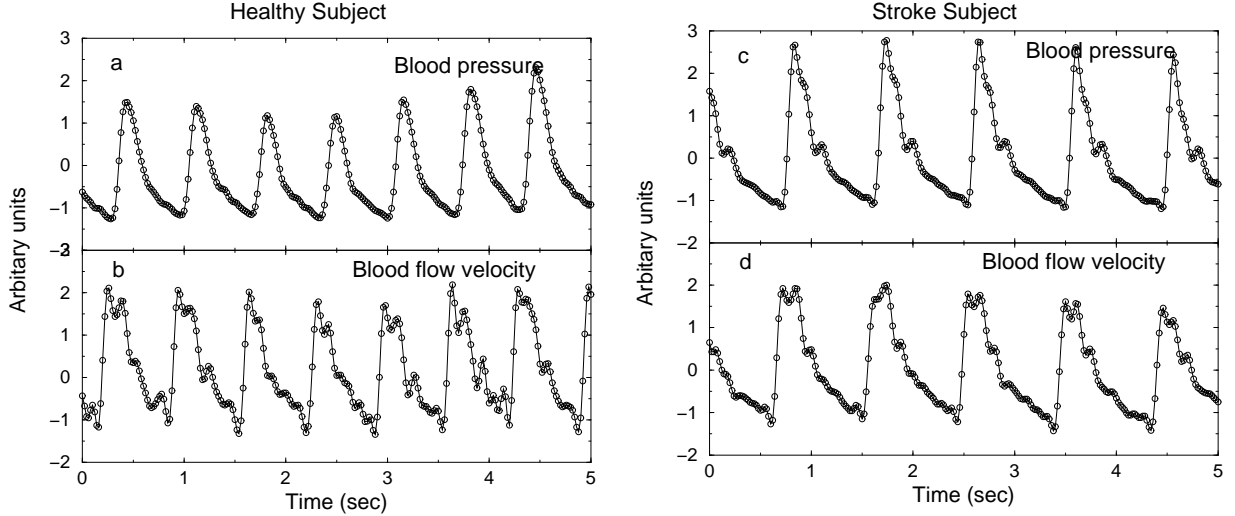


FIG. 1: BFV and BP signals during CO₂ re-breathing stage after a band-pass Fourier filter in the range [0.05Hz, 10Hz] and normalization to unit standard deviation: (a-b) for a healthy subject, (c-d) for a post-stroke subject.

as

$$H(f) = \frac{S_{PV}(f)}{S_{PP}(f)}. \quad (2)$$

From the real part $H_R(f)$ and imaginary part $H_I(f)$ of the transfer function, we can obtain its amplitude (also called gain) $|H(f) = [H_R^2(f) + H_I^2(f)]^{1/2}|$ and its phase $\Phi(f) = \arctan[H_I(f)/H_R(f)]$. We note that the phase $\Phi(f)$ is a frequency domain characteristic of the cross-spectrum between two signals, and is different from the instantaneous phase in the time domain we discuss in the next section.

Phase synchronization

We study beat-to-beat BP-BFV interaction during quasi-steady state conditions (supine, upright tilt, upright hyperventilation and CO₂ rebreathing [Fig 1(a) and (b)] employing a phase synchronization method. We first apply a high-pass ($f > 0.05\text{Hz}$) and a low-pass ($f < 10\text{Hz}$) Fourier filter to the BFV and BP signals. The high-pass filter is used to reduce the nonstationarity in the signals. The low-pass filter is used to remove high frequency random fluctuations in the signals. Next we perform the Hilbert Transform which for a time series $s(t)$ is defined as [24, 25, 29, 30, 31]

$$\tilde{s}(t) = \frac{1}{\pi} P \int_{-\infty}^{\infty} \frac{s(\tau)}{t - \tau} d\tau, \quad (3)$$

where P denotes Cauchy Principal value. $\tilde{s}(t)$ has an apparent physical meaning in Fourier space: for any positive (negative) frequency f , the Fourier component of the Hilbert transform $\tilde{s}(t)$ at this frequency f can be obtained from the Fourier component of the original signal $s(t)$ at the same frequency f after a 90° clockwise (anti-clockwise) rotation in the complex plane. For example,

if the original signal is $\sin at$, its Hilbert transform will become $\cos at$. For any signal $s(t)$ one can always construct its “analytic signal” S [24, 25, 29, 30, 31], which is defined as

$$S \equiv s(t) + \tilde{s}(t) = A(t)e^{i\varphi(t)}, \quad (4)$$

where $A(t)$ and $\varphi(t)$ are the instantaneous amplitude and phase of $s(t)$, respectively. The amplitude $A(t)$ and the phase $\varphi(t)$ are instantaneous characteristics of a time series $s(t)$, and present different aspects of the signal. For a pure sinusoid, the instantaneous amplitude is a constant and the instantaneous phase is a straight line over time: the amplitude quantifies the strength of the oscillation and the slope of the straight line quantifies how fast is the oscillation. For more complex signals, both the instantaneous amplitude and phase may display complicated forms. We note that, the result of the Hilbert transform does not depend on the mean of the original signal $s(t)$, thus for two signals $s(t)$ and $s(t) + \text{const}$, one will obtain identical values for $\tilde{s}(t)$. However, such a shift in the mean value of $s(t)$ will affect the amplitude $A(t)$ and the phase $\varphi(t)$ of the analytical signal. Since we have first applied a high-pass filter in the frequency domain ($f > 0.05 \text{ Hz}$), the mean of $s(t)$ becomes zero and the instantaneous amplitude and phase we obtained are uniquely defined. Further we note that the instantaneous phase $\varphi(t)$ is different from the transfer function phase $\Phi(f) - \varphi(t)$ is a time domain characteristic of a single signal, while $\Phi(f)$ is a cross-spectrum characteristic of two signals in the frequency domain.

The instantaneous phase $\varphi(t)$ for both BFV and BP is a nonstationary signal and can be decomposed into two parts: a linear trend and fluctuations along the trend. The trend is mainly driven by the periodic heart rate at a frequency $\approx 1 \text{ Hz}$. However, the fluctuations are of specific interest since they may be affected by the cere-

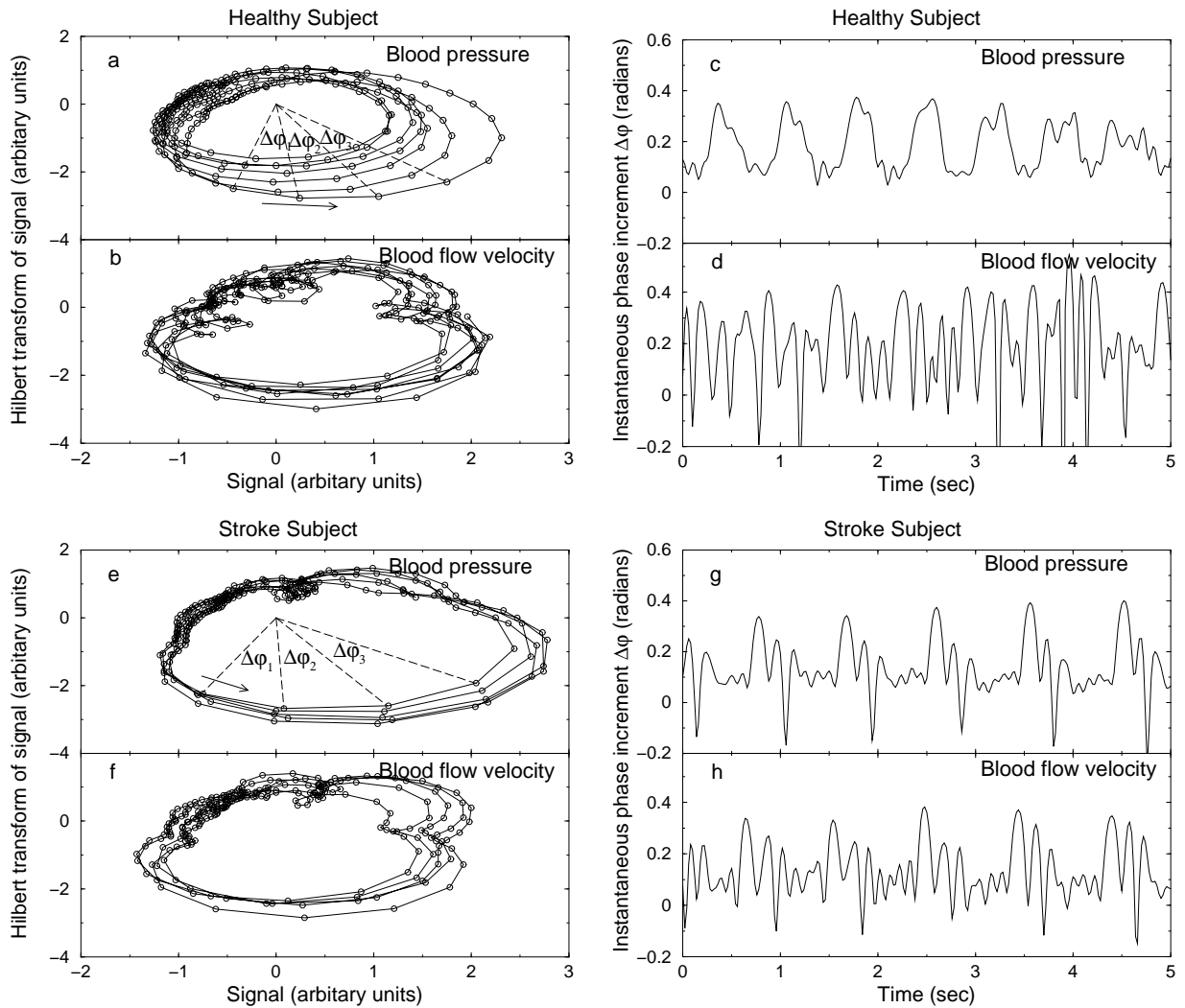


FIG. 2: Presentation of the BFV and BP signals vs. their Hilbert transforms (a-b) and their corresponding instantaneous phase increment $\Delta\varphi$ during the CO₂ re-breathing condition (c-d) for the same data from a healthy subject as shown in Fig. 1a-b. BFV and BP signals vs. their Hilbert transforms (e-f) and their corresponding instantaneous phase increment $\Delta\varphi$ during the CO₂ re-breathing condition (g-h) for the same data from a stroke subject as shown in Fig. 1c-d. Repetitive temporal patterns associated with each heartbeat in $\Delta\varphi$ for the BP signal from a healthy subject (c) are not matched by corresponding patterns in the BFV signal (d), reflecting active cerebral vascular regulation. In contrast, periodic patterns in $\Delta\varphi$ of the BP signal from a stroke subject (g) are matched by practically identical patterns in $\Delta\varphi$ of the BFV signal (h), indicating dramatic impairment of cerebral vascular tone with higher vascular resistance after minor ischemic stroke.

bral autoregulation. To remove the trend, we consider the increments in the consecutive values of the instantaneous phase, defined as $\Delta\varphi(t_i) = \varphi(t_i) - \varphi(t_{i-1})$, where t_i and t_{i-1} are the time corresponding to two successive recordings (in our case we have $t_i - t_{i-1} = 0.02\text{sec}$). The instantaneous phase increment signal $\Delta\varphi$ is stationary, and fluctuates in the range $(-\pi, \pi)$. In Fig. 2 (c-d) we show examples of $\Delta\varphi$ for healthy subjects and in Fig. 2 (g-h) for stroke subjects.

We then apply a cross-correlation analysis to quantify the dynamical relationship between the stationary phase increments $\Delta\varphi$ of the BFV and BP signals. For each subject, during each one of the four physiologic condi-

tions we calculate the correlation coefficient $C(\tau)$ vs. the time lag τ between the BFV and BP signals. To quantitatively distinguish the control group and the stroke group, we further analyze the characteristics of the correlation function $C(\tau)$. Specifically, we investigate the maximum value of $C(\tau)$, denoted as C_{max} , which represents the strength of the cross-correlation between the instantaneous phases of the BFV and BP signals. Another important characteristic of the cross-correlation function is how fast the correlation between two signals decreases for increasing values of the time lag τ . To quantify this aspect, we choose a fixed threshold value, $r = 0.3$, which is the same for all subjects. Since $C(\tau)$ is a periodic-like

function of the time lag τ with a decreasing amplitude for increasing τ (Fig. 3), we first record all maxima of $|C(\tau)|$ during each heart beat period (~ 1 sec), then we determine the two maxima with largest positive and negative time lags τ at which the correlation function $C(\tau)$ is above rC_{max} . The average of the absolute values for these two time lags is marked as a characteristic time lag τ_0 .

III. RESULTS

Mean values.

We compare the mean values of all signals for both control and stroke groups and for all four conditions (baseline, upright tilt, tilt-hyperventilation and CO₂ rebreathing) and groups (control and stroke) using MANOVA. Results are shown in Table I. We find that the mean values of the BFV and CO₂ signals are significantly different for the four different conditions while the BP signal has a mean value similar for all four conditions. For control and stroke group comparison, we find that BFVs from the left (stroke side) MCA were significantly different, and that the mean value of BP for the stroke group is significantly higher than that for control group. Furthermore, we observe that the cerebral vascular resistance (CVR) is significantly higher for the stroke group.

Transfer function analysis.

We apply transfer function analysis on the original BFV and BP signals under different tests in both the low frequency (LF) LF (0.05-0.2 Hz) and the heart beat frequency (HBF) (0.7-1.4 Hz) range. Gain, phase and coherence are calculated for each subject and for all four physiologic conditions (Table II). We use MANOVA to compare our results for the two groups and for the four conditions. In both frequency ranges, we do not find significant difference in the gain. In the LF range, phase $\Phi(f)$ and coherence $\gamma^2(f)$ are significantly different between the tests, but are not different between the groups. In the HBF range, we find that the phase $\Phi(f)$ for the MCAL-BFV is significantly different between the conditions ($p=0.03$). The coherence in the HBF range shows no significant difference in the tests comparison, however, it is significantly higher for the control group.

Phase synchronization analysis.

We apply the phase synchronization analysis to all four conditions and both study groups. We find that the patterns of cross-correlation function $C(\tau)$ of the instantaneous phase increments $\Delta\varphi$ of the BFV and BP signals are very different for the stroke group compared to the control group. In general, the cross-correlation function $C(\tau)$ for the control group is characterized by smaller amplitude and faster decay (time lag τ less than 10 secs) [Fig. 3]. In contrast, for stroke subjects, the amplitude of the cross-correlation function $C(\tau)$ has much larger amplitude and decays much slower (over time lags larger than 10 secs) [Fig. 3]. Because of the strong correlation between BFV and BP signals, for those stroke patients

the changes of the phase of BFV will change in the approximately same way with that of BP signals, indicating a strong synchronization.

The correlations at short time scales (less than 10 seconds) may be partially attributed to the effect of heart rate (~ 1 sec) and respiration (~ 5 secs)— i.e., they reflect the effect of other body regulations (similar to “background noise”) on both BFV and BP signals. When cerebral autoregulation is effective, because of its fast-acting mechanism [3], it may also contribute to the significantly weaker cross-correlations at short time scales we find in healthy subjects compared to post-stroke subjects (Fig. 3). However, the correlation due to the above mechanisms will decrease very fast when increasing the time lag τ between BFV and BP signals. Thus, the correlations at long time scales (>10 secs) observed for stroke subjects (Fig. 3), cannot be attributed to the effect of cerebral autoregulation. Instead, the existence of such strong and sustained cross-correlations may imply that BFV will passively follow the changes of BP, thus indicating absence of vascular dilation or constriction and impaired cerebral autoregulation for the stroke subjects.

To quantitatively distinguish control group and stroke group, we have studied the characteristics of the correlation function $C(\tau)$ for all subjects. For each correlation function $C(\tau)$, we first find C_{max} , the maximal value of $C(\tau)$, which tells the strength of the correlation. Then we choose a threshold value, e.g., $r = 0.3$, search for the maximum of $|C(\tau)|$ during each heart beat period along both positive and negative lags, and find two points in those maxima with largest time lags at which the correlation are still above rC_{max} . The average of absolute values of these two points gives the characteristic time lags τ_0 . From τ_0 and C_{max} for all subjects and during all tests, one can confirm that the stroke group tends to have larger C_{max} and longer time lag τ_0 compared to those for the control group.

We have applied MANOVA to demonstrate whether τ_0 and C_{max} are different for control subjects and stroke patients. The results are shown in Table III. We find that during tilt and hyperventilation tests, control and stroke group indicate no significant difference (p values > 0.05). In contrast, in supine and CO₂ re-breathing tests, the difference between the control group and the stroke group becomes significant (p values < 0.05).

To explain the above difference in τ_0 and C_{max} in the supine stage, we note that stroke group had higher BP and CO₂ in baseline (see Table I). Therefore, BP autoregulatory curve for the stroke subjects was shifted to the right or higher BP values while the plateau of this curve was already narrowed because of the higher level of CO₂ [3]. Tilt CO₂ rebreathing increased CO₂ after a period of hypocapnia, thus further tested the CO₂ reactivity and showed impaired vasodilatory responses in stroke subjects. In contrast, vasoconstrictor responses to tilt-up hyperventilation were preserved.

Frequency Range	Variable		Supine		Tilt		Hyperventilation		CO ₂ rebreathing		Statistics	
			MCAR-BFV	MCAL-BFV	MCAR-BFV	MCAL-BFV	MCAR-BFV	MCAL-BFV	MCAR-BFV	MCAL-BFV	MCAR-BFV	MCAL-BFV
LF 0.05-0.2Hz	Gain	Control	0.94±0.30	0.97±0.27	1.06±0.21	0.97±0.21	0.95±0.41	1.02±0.43	1.03±0.15	1.03±0.15	0.38*	0.11*
		Stroke	0.84±0.42	0.72±0.37	0.95±0.27	0.95±0.25	1.09±0.36	1.08±0.38	0.92±0.20	0.95±0.21	0.48 ⁺	0.26 ⁺
	Coherence	Control	0.65±0.15	0.59±0.21	0.75±0.08	0.66±0.19	0.58±0.18	0.62±0.19	0.82±0.09	0.84±0.08	0.0006*	0.0004*
		Stroke	0.53±0.19	0.44±0.24	0.70±0.20	0.66±0.27	0.62±0.17	0.61±0.19	0.69±0.19	0.70±0.20	0.07 ⁺	0.07 ⁺
	Phase	Control	0.56±0.27	0.63±0.26	0.62±0.32	0.63±0.30	0.92±0.33	0.94±0.39	0.63±0.23	0.63±0.20	0.0002*	0.0001*
		Stroke	0.79±0.27	0.56±0.38	0.58±0.24	0.60±0.25	0.86±0.32	0.94±0.47	0.42±0.25	0.49±0.23	0.74 ⁺	0.37 ⁺
HBF 0.7-1.4Hz	Gain	Control	0.92±0.18	0.93±0.24	0.91±0.15	0.91±0.21	0.88±0.23	0.94±0.23	0.89±0.16	0.91±0.18	0.50*	0.73*
		Stroke	0.77±0.29	0.82±0.28	0.88±0.27	0.97±0.43	0.97±0.24	0.98±0.28	0.96±0.28	0.97±0.31	0.96 ⁺	0.84 ⁺
	Coherence	Control	0.76±0.15	0.75±0.18	0.75±0.13	0.71±0.18	0.58±0.16	0.58±0.18	0.68±0.23	0.70±0.22	0.15*	0.27*
		Stroke	0.64±0.24	0.63±0.25	0.57±0.23	0.56±0.21	0.55±0.20	0.56±0.21	0.64±0.25	0.63±0.27	0.035 ⁺	0.05 ⁺
	Phase	Control	0.32±0.13	0.27±0.14	0.38±0.18	0.38±0.20	0.46±0.27	0.46±0.26	0.46±0.26	0.42±0.24	0.16*	0.03*
		Stroke	0.35±0.31	0.31±0.24	0.36±0.14	0.36±0.21	0.47±0.20	0.49±0.28	0.42±0.21	0.42±0.15	0.95 ⁺	0.81 ⁺

* P value between tests comparisons

+ P value between groups comparisons

TABLE II: Gain and coherence in the LF (0.05-0.2 Hz) and HBF (0.7-1.4 Hz) frequency ranges between control and stroke groups during different tests. The p values from 2x4 MANOVA are calculated for comparing groups and tests difference.

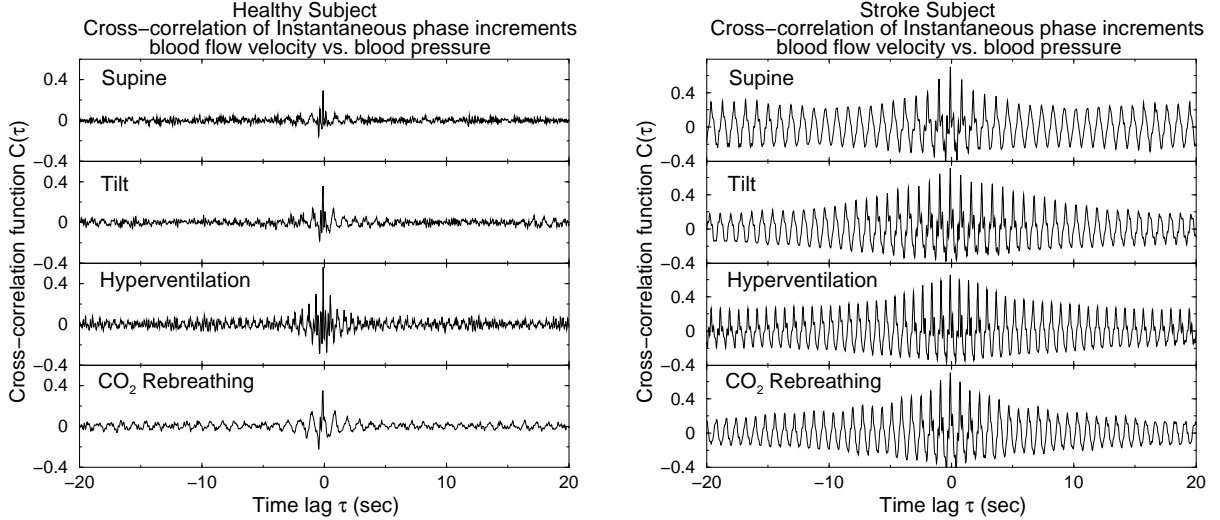


FIG. 3: Cross-correlation function $C(\tau)$ of the instantaneous phase increment $\Delta\varphi$ for the BFV and BP signals during four physiologic conditions. We find that the cross-correlation function for all healthy subjects exhibits a very distinct type of behavior compared to stroke subjects. Two typical examples are shown (Left) A healthy subject: $C(\tau)$ has a small amplitude at $\tau = 0$ and is close to zero at time lags $\tau < 5$ secs., during all four conditions. (Right) A stroke patient: $C(\tau)$ has a much larger amplitude at $\tau = 0$ which lasts for lags τ up to 20 seconds, indicating a strong synchronization between the BFV and BP signals, i.e., loss of cerebral autoregulation.

Variable		Supine		Tilt		Hyperventilation		CO ₂ rebreathing		Statistics	
		MCAR-BFV	MCAL-BFV	MCAR-BFV	MCAL-BFV	MCAR-BFV	MCAL-BFV	MCAR-BFV	MCAL-BFV	MCAR-BFV	MCAL-BFV
C_{max}	Control	0.55±0.17	0.49±0.22	0.39±0.16	0.33±0.17	0.47±0.17	0.43±0.16	0.45±0.13	0.41±0.13	0.006*	0.07*
	Stroke	0.62±0.12	0.58±0.14	0.43±0.21	0.47±0.20	0.51±0.19	0.52±0.20	0.57±0.20	0.58±0.21	0.049 ⁺	0.001 ⁺
τ_0	Control	2.0±2.0	2.0±1.7	2.2±1.3	2.5±1.5	2.0±0.9	2.0±0.9	2.6±1.5	2.6±1.5	0.6*	0.7*
	Stroke	6.6±6.7	5.9±5.3	3.8±3.4	3.6±3.5	5.3±5.6	5.7±5.9	5.9±5.4	5.8±5.6	0.0003 ⁺	0.0004 ⁺

* P value between tests comparisons

+ P value between groups comparisons

TABLE III: The maximum correlation strength C_{max} and the characteristic lag τ_0 between control and stroke groups during different conditions. The p values from 2x4 MANOVA are calculated for comparing groups and tests difference.

IV. CONCLUSIONS

In this study we investigate dynamics of cerebral autoregulation from relationship between BP and BFV signals in control and stroke groups. We compare the statistical properties of BFV and BP signals as well as the synchronization between them. We evaluate the combined effects of pressure autoregulation (upright tilt) and metabolic autoregulation (hyperventilation and CO₂ rebreathing) in healthy and post-stroke subjects. We apply a synchronization method (based on the Hilbert transform) to quantify the possible phase relations between the BFV and BP signals. We find that the cross-correlation between the instantaneous phase increments obtained from the BFV and BP signals provides insight into the dynamics of BP-BFV regulation in healthy and post-stroke subjects. Our results for stroke patients show a stronger and more sustained synchronization between BFV and BP signals in supine and CO₂ rebreathing, which cannot be simply explained by heart rate and/or respiration. Such robust synchronization pattern is not apparent in control subjects, and indicates impaired cere-

bral autoregulation for chronic stroke patients. Stronger BP-BFV synchronization in the stroke subjects may reflect higher vascular resistance and the effects of slower vasomotor BP rhythms on cerebral blood flow. In the controls, these effects may be attenuated by the myogenic regulation. This synchronization method enables to assess dynamics of phase relationship on a beat-to-beat basis that can be applied to assess dynamics of vasoregulation.

Acknowledgments

Z.C., K.H., H.E.S., and P.Ch.I. acknowledge support from NIH Grant No. HL071972 and NIH/National Center for Research Resources Grant No. P41RR13622. V.N. acknowledges support from American Heart Foundation Grant No. 99 30119N, 1R01 NIH-NINDS (1R01-NS045745-01), NIH GCRC Grant 5 MOIRR00034 and MO1-RR01302, and The Older American Independence Center Grant 2P60 AG08812-11.

-
- [1] N. A. Lassen, *Physiol. Rev.* **39**, 183, 1959.
 - [2] K. Narayanan, J. J. Collins, J. Hammer, S. Mukai, and L.A. Lipsitz, *Am. J. Physiol. Regulatory Integrative Comp. Physiol.* **281**, R716, 2001.
 - [3] R. B. Panerai, *Physiol. Meas.* **19**, 305, 1998.
 - [4] S. Schwarz, D. Georgiadis, A. Aschoff, and S. Schwab, *Stroke* **33**, 497, 2002.
 - [5] P. J. Eames, M. J. Blake, S. L. Dawson, R. B. Panerai, and J. F. Potter, *J. Neurol. Neurosur. Ps.* **72**, 467, 2002.
 - [6] V. Novak, A. Chowdhary, B. Farrar, H. Nagaraja, J. Braun, R. Kanard, P. Novak, and A. Slivka, *Neurology* **60**, 1657, 2003.
 - [7] V. Novak, A. C. Yang, L. Lepicovsky, A. L. Goldberger, L. A. Lipsitz, and C.-K. Peng, *BioMedical Engineering online* **3**, 39, 2004.
 - [8] S. S. Kety, and C. F. Schmidt, *J. Clin. Invest.* **29**, 476, 1948.
 - [9] W. D. Obrist, H. K. Thompson, H. S. Wang, and W. E. Wilkinson, *Stroke* **6**, 245, 1975.
 - [10] R. Aaslid, K. F. Lindegaard, W. Sorteberg, and H. Nornes, *Stroke* **20**, 45, 1989.
 - [11] F. P. Tiecks, A. M. Lam, R. Aaslid, and D. W. Newell, *Stroke* **26**, 1014, 1995.
 - [12] S. L. Dawson, M. J. Blake, R. B. Panerai, and J. F. Potter, *Cerebrovasc. Dis.* **10**, 126, 2000.
 - [13] R. B. Panerai, S. L. Dawson, P. J. Eames, and J. F. Potter, *Am. J. Physiol. Heart Circ. Physiol.* **280**, H2162, 2001.
 - [14] C. Hugenii, *Horoloquim Oscilatorium* (Parisiis, France, 1673).
 - [15] L. Fabiny, P. Colet, R. Roy, and D. Lenstra, *Phys. Rev. A* **47**, 4287, 1993; R. Roy, and K. S. Thornburg, *Phys. Rev. Lett.* **72**, 2009, 1994.
 - [16] V. S. Anischenko, T. E. Vadivasova, D. E. Postnov, and M. A. Safonova, *Int. J. Bifurcation Chaos Appl. Sci. Eng.* **2**, 633, 1992.
 - [17] J. F. Heagy, T. L. Carroll, and L. M. Pecora, *Phys. Rev. A* **50**, 1874, 1994.
 - [18] I. Schreiber, and M. Marek, *Physica (Amsterdam)* **5D**, 258, 1982; S. K. Han, C. Kurrer, and Y. Kuramoto, *Phys. Rev. Lett.* **75**, 3190, 1995.
 - [19] S. Bahar, A. Neiman, L. A. Wilkens, and F. Moss, *Phys. Rev. E* **65**, 050901, 2002.
 - [20] D. Rybski, S. Havlin, and A. Bunde, *Physica A* **320**, 601, 2003.
 - [21] S. Bahar, and F. Moss, *Chaos* **13**, 138, 2003.
 - [22] A. S. Pikovsky, *Radiophys. Quantum Electron.* **27**, 576, 1984.
 - [23] Y. Kuznetsov, P. Landa, A. Ol'khovoi, and S. Perminov, *Sov. Phys. Dokl.* **30**, 221, 1985.
 - [24] M. G. Rosenblum, A. S. Pikovsky, and J. Kurths, *Phys. Rev. Lett.* **76**, 1804, 1996.
 - [25] M. G. Rosenblum, A. S. Pikovsky, and J. Kurths, *Phys. Rev. Lett.* **78**, 4193, 1997.
 - [26] U. Parlitz, L. Junge, W. Lauterborn, and L. Kocarev, *Phys. Rev. E* **54**, 2115, 1996.
 - [27] S. Bahar, *Fluc. Noise Lett.* **4**, L87, 2004.
 - [28] C. Schafer, M. G. Rosenblum, J. Kurths, H. H. Abel, *Nature (London)* **392**, 239, 1998.
 - [29] J. F. Claerbout, *Fundamentals of Geophysical Data Processing* (McGraw-Hill, New York, 1976).
 - [30] A. V. Oppenheim, and R. W. Schafer, *Discrete-Time signal Processing, 2nd ed.* (Prentice-Hall, UpperSaddle River, New Jersey, 1998).
 - [31] S. L. Marple, *IEEE T. Signal Proces.* **47**, 2600, 1999.
 - [32] R. B. Panerai, S. L. Dawson, and J. F. Potter, *Am. J. Physiol. Heart Circ. Physiol.* **277**, H1089, 1999.